

UC Berkeley

UC Berkeley Previously Published Works

Title

Origin, structure, and role of background EEG activity Part 3. Neural frame classification

Permalink

<https://escholarship.org/uc/item/8z1201cb>

Journal

Clinical Neurophysiology, 116(5)

Author

Freeman, Walter J, III

Publication Date

2005

Peer reviewed

Origin, structure, and role of background EEG activity

Part 3. Neural frame classification

Walter J Freeman

Department of Molecular & Cell Biology, LSA 142
University of California
Berkeley CA 94720-3200 USA
Tel. 1-510-642-4220 Fax 1-510-643-6791

<http://sulcus.berkeley.edu>
wfreeman@socrates.berkeley.edu

Running title: Neural frame classification

Key words: amplitude patterns, beta-gamma oscillations, binding, cinematographic dynamics, field theory, neural frame, pragmatic information, spatial EEG analysis

Clinical Neurophysiology (2004): accepted 29 December 2004.

Acknowledgments

This study was partially supported by grants MH 06686 from the National Institute of Mental Health, NCC 2-1244 from the National Aeronautics and Space Administration, and EIA-0130352 from the National Science Foundation to Robert Kozma. Programming was by Brian C Burke. Essential contributions to surgical preparation and training of animals, data acquisition, and data analysis by John Barrie, Gyöngyi Gaál, and Linda Rogers, and the assistance of Prof. Andreas König, Technische Universität Kaiserslautern are gratefully acknowledged. The rabbit EEG data used in this study are available to scientists associated with The Brain Resource International Database <<http://www.BrainResource.com>> and Brain Dynamics Centre

<<http://www.Brain-Dynamics.org>>. This report is dedicated to the memory of Linda Rogers.

Abstract

Objective: To show that cortical responses to conditioned stimuli (CS) include intermittently induced spatial patterns of amplitude modulation (AM) of beta-gamma oscillation called frames.

Methods: EEGs were recorded from 8x8 high-density arrays fixed on primary sensory cortices of rabbits trained to discriminate CS with reinforcement (CS+) from those without (CS-). EEG frames were located with a pragmatic information index, H_e . The spatial patterns of the first 3 frames on each of 37-40 trials were measured by the square of 64 analytic amplitudes from the Hilbert transform to give points in 64-space. The questions were asked: Did the frames from CS+ trials and CS- trials differ within each sequential group? Did the three frames differ from each other (form 3 clusters of points)?

Results: EEG frames that were identified by high H_e had AM patterns that could be classified with respect to CS+ and CS- well above chance levels. Two stages of correct frame classification occurred on each trial: 40-130 ms after CS onset with a gamma carrier frequency, and 450-550 ms with a beta carrier frequency. Peak power in the beta frames was double that in gamma frames, and mean pattern surface area of beta frames was nearly four-fold greater.

Conclusions: Under the impact of a CS on a sensory neocortex the background EEG activity reorganized in sequential frames of coordinated activity, first local and modality-specific, thereafter global.

Significance: The size, texture and duration of these AM patterns indicate that spatial patterns of human beta frames may be accessible with high-density scalp arrays for correlation with phenomenological reports by human subjects.

1. Introduction

The intent of this tripartite study is to develop a way to think about neocortex that can describe and explain its capacity for rapid, global integration in perception. The problem is exemplified by human and animal behaviors in which the glimpse of a face, the crack of a twig, or the scent of food or perfume can in a fraction of a second galvanize virtually the entire body into directed action or the preparation for action that is based selectively in previous experience. How is it that the sensory impact of a few molecules, photons and phonons onto a prepared brain can be amplified into the coordinated activity of the entire forebrain in literally the time needed to blink an eye? The way proposed here to answer this question is to analyze, classify, and interpret the spatial patterns of EEGs from high-density arrays of electrodes on rabbit, gerbil, and cat neocortex, because their textures have been found to be related to categories of simple stimuli that the subjects had learned to perceive through classical and operant conditioning [Barrie, Freeman and Lenhart, 1996; Ohl, Scheich and Freeman, 2001; Freeman, Gaál and Jornten, 2003].

During an act of perception, the forebrain has been described as generating a sequence of active states that can be conceived as frames that constitute a sequence of points in a step-wise trajectory through an infinite-dimensional brain state space [Freeman, 2003a,c]. This discontinuous mode of function has been described as “cinematographic” [Sacks, 2004]. Measurement and analysis of multiple EEGs from an electrode array on a brain surface gave a sequence of points that constituted the projection of a staccato trajectory into a finite n -dimensional subspace, where n was the number of electrodes, here 64. Visualization was by further reduction into 2-space using a variety of multivariate statistical techniques for clustering including nonlinear mapping [Sammon, 1969]. Clusters of points in n -space to which a brain returned repeatedly and reliably (for example, the two clusters in Fig. 3, D) defined a transiently ‘stable’ brain state that constituted a cinematographic ‘frame’. Some properties derived for a frame were the time interval needed for its onset; its latency and duration in ms; its diameter in mm; its peak power; the spectral range of its carrier wave in Hz; its spatial patterns of analytic amplitude modulation (AM) and phase modulation (PM); and the behavioral correlates, if any, of its AM patterns.

A sequence of AM patterns in frames formed an itinerant trajectory [Tsuda, 1961] in a subspace of brain state space; the sequence was regarded as a precursor of perception. Studies of the process of perception consisted of measurement and classification of the AM patterns in sensory cortical frames that accompanied behavioral discrimination of conditioned stimuli (CS). In these sequential cortical frames from high-density EEG arrays [Freeman and Grajski, 1987; Grajski and Freeman, 1989; Freeman and Van Dijk, 1987; Barrie, Freeman and Lenhart, 1996; Ohl, Scheich and Freeman, 2001; Freeman and Burke, 2003] a significant level of correct classification of AM patterns occurred in 1 to 3 time periods starting soon after CS arrival. Maximal classification was usually found in the first period within 40-130 ms of CS onset. The reduced level of correct classification in later periods was attributed to greater variation in the onset latencies of frames in the 37-40 trials in each session, variation that Tallon-Baudry et al. [1996] termed ‘jitter’. Modest improvement in classification rates was obtained by systematic variation of the onset times of the samples from the sets of trials about the mean onset time across all trials [Freeman, 2003b], or by measurement of the spatial patterns of phase modulation

(PM) of the beta-gamma oscillations as markers for the location of frames related to the CS+ and CS- [Freeman and Barrie, 2000; Freeman, 2003b].

Recent advances in application of the Hilbert transform to EEGs in the beta and gamma ranges [Freeman, 2004a] led to the detection in the EEG of spatial AM patterns having high degrees of coherence, stability, and intensity. These epochs were identified with high values of an index, H_c , that Atmanspacher and Scheingraber [1991] labeled ‘pragmatic information’. The epochs with high H_c appeared on average to correspond in location and duration to the peaks of high levels of correct classification determined by the Euclidean distance between points in 64-space [Barrie, Freeman and Lenhart, 1996]. The latencies and durations of epochs varied across trials. The hypothesis is proposed here that the segments identified by high H_c will serve to locate frames that have optimal classification with respect to the CS+ and CS- and therefore have maximal information.

Furthermore, the aspect has been emphasized [Freeman, 2003a, 2004a] that the term “information” is directed not to the brain activity that implements meaning which is not information, rather to the digitized EEG numbers that contain information but have no meaning. Clearly brain information must be traced ultimately to the environment. It is well understood that information in a sensory stimulus is transformed by receptors first into generator currents and then into action potentials. These pulse trains convey the information through further transformations by intervening relays to the cortex, where it is injected and can be partially retrieved by time-locked averaging of multiple cortical responses to the stimulation. However, it is not the case that the relayed information is simply transformed into the non-averaged pattern of cortical activity on individual trials whereby feature binding occurs [Singer and Gray, 1995; Engel, Fries and Singer, 2001]. Rather the observed pattern is a transformation of the preceding background cortical pattern through a state transition, by which the stimulus selects a basin of attraction from an attractor landscape. The selected attractor shapes a new pattern that incorporates as a small contribution the relayed information carried by the action potentials that initiated the state transition. Owing to the predominance of synapses from axons of cortical origin over those from afferent axons, the pragmatic information observed in each single-trial pattern is shaped mainly by the selected attractor and only secondarily by the new information that through one-trial learning modifies the attractor landscape and up-dates it. The experimental evidence is the lack of invariance with respect to fixed CS and the context dependence of CS-related cortical patterns. The basin of attraction provides for generalization to a category, and the attractor provides for abstraction by which cortical output signals the class to which a stimulus belongs, and which may appear as feature binding. In the event of repeated nonconvergence constituting failure to select the basin of an existing attractor, a higher-order state transition may initiate formation of a new basin of attraction [Kozma and Freeman, 2001] corresponding to the inception of a new category of stimulus through insight learning [Ohl, et al., 2003]. In either case the application of information theory to measure the content of successive cortical patterns is expected to reveal growth, compared with Shannonian entropic decay expected for cortical readings of thalamic messages.

The test of the hypothesis described in this study is complicated by three factors. First, many frames appear to have no demonstrable correlation with the CS, even when they occur in the interval between onsets of the CS and the CR. Second, the several parameters of the analysis

appear to interact, yet the cumbersome technique of classifier-directed optimization to extract the behaviorally related information allows systematic change in only one parameter at a time. Third, the classifiability of frames is shown to be frequency-dependent. Whereas root mean square (rms) amplitudes can be calculated across frequency ranges of any width, calculation of analytic amplitudes by the Hilbert transform for classification requires modest temporal band pass filtering. The H_c frames with earlier latencies that gave optimal classification are shown to have carrier frequencies in the gamma range, whereas frames with longer latencies have carrier waves in the beta range. The classification of H_c frames here is by nonlinear mapping [Sammon, 1969; Barrie, Holcman and Freeman, 1999; König, 2000] preceding and including the previous technique of calculating centers of gravity and Euclidean distances in n-space because of its greater flexibility in distinguishing frames on CS+ trials from frames on CS- trials in any order, as well as sequential frames on the same trials. Unfortunately, neither method supports classification across distinctive frequency ranges in a single step. Finally, theoretical considerations in deriving H_c [Freeman, 2004a] require the calculation of power, A^2 , as distinct from amplitude, A . Fortunately the use of A^2 is found empirically to give rates of correct classification superior to those from using A . The results demonstrate the value of the index H_c for locating frames of beta and gamma activity that are significantly related to behavior.

2. Methods

2.1. Subjects, data collection and preprocessing

Rabbits were implanted each with an 8x8 electrode array having average spacing of 0.79 mm and giving a window onto a cortical surface of 5.6x5.6 mm. Data from 2 visual, 3 somatic, and 4 auditory cortices [Barrie, Freeman and Lenhart, 1996] were used in this study. Two visual replicates and one somatic replicate were included for statistical purposes. The rabbits had been trained to discriminate conditioned stimuli in the appropriate modality in a classic aversive paradigm with reinforcement by a weak electric shock to the cheek as the unconditioned stimulus (US). The visual CS was a weak or a strong full field flash. The somatic stimulus was a puff of air to the face or to the lumbar region. The auditory stimulus was a brief tone at 500 Hz or 5000 Hz. The data for each rabbit consisted of 37 to 40 trials with random alternation of CS+ and CS- presentations. Each trial lasted 6 s with onset of a CS at 3 s that ended the control period and began the test period and the US ended the test period. The 64 EEGs were analog filtered at 0.1 and 100 Hz, amplified 10K, digitized in 12 bits at 2 ms intervals, and stored in 37-40 blocks of 3000x64 time series. All computations were done with a MATLAB 6.5 software package [Mathworks, Inc., Natick, MA].

2.2. Location of stable AM patterns of high intensity using the Hilbert transform

Seven steps (Fig. 1, A, upper trace) were required to localize frames in which to calculate feature vectors for classification. Step 1: The time series from each channel was demeaned to remove channel bias, and the entire trial set of blocks (40x3000x64) was normalized by dividing all EEG amplitudes by the global standard deviation (SD, lower trace). Step 2: The 64 amplitudes at each

digitizing step in all 37-40x3000 blocks were spatially low pass filtered (Fig. 1, A, lower trace) with a 2-D Gaussian filter [Freeman, 2004a, Appendix 1, B]. Step 3: The 37-40x64 EEG signals in 3000 time steps were band pass filtered by convolution in the time domain (Fig. 1, B, middle trace) with finite impulse response (FIR) filters using Parks-McClellan algorithm of order 200 and transition bandwidth 4 Hz. [Freeman, 2004a, Appendix 1, A].

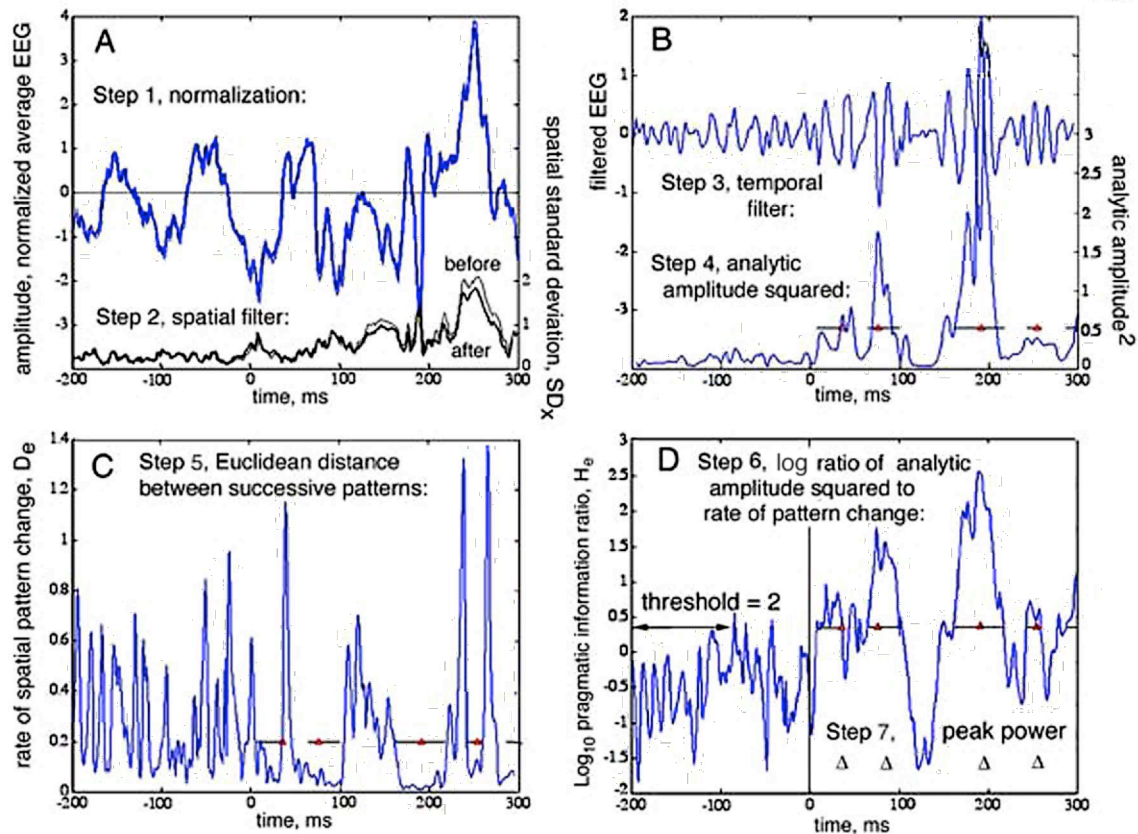


Fig. 1. The algorithms are illustrated that were used to locate each stable spatial frame in which to calculate its feature vector for classification. **A.** Average (upper curves) and SD (lower curves) of 64 EEGs from one trial in a 500 ms segment extending across CS arrival at 0 ms; Step 1, after channel demeaning and amplitude normalization; Step 2, before and after low pass spatial filtering at 0.3 c/mm.

B. Upper curve: Step 3, average EEG after temporal band pass filtering at 20-80 Hz. Lower curve: Step 4, spatial average, $\underline{A}^2(t)$, of the analytic amplitude squared, $A_j^2(t)$, averaged over channels, $j = 1, 64$, at each digitizing step, t . The increase in $\underline{A}^2(t)$ was not due to an increase in synchrony, which was shown to increase to a maintained level before $\underline{A}^2(t)$ began to rise [Freeman, 2004a].

- C.** Step 5: The 64 values of $A_j^2(t)$ gave a 1x64 feature vector, $\mathbf{A}^2(t)$, that specified an AM pattern and a point in 64-space. The Euclidean distance, D_e , between successive points, $\mathbf{A}^2(t) - \mathbf{A}^2(t-1)$, gave the rate of change in the AM pattern. Successive low values indicated pattern stability.
- D.** Step 6: The pragmatic information was given by the ratio $H_e = \underline{\mathbf{A}}^2(t)/D_e(t)$. Qualifying segments were identified by the criteria that H_e remained above a threshold, here $t_e = 2$, longer than a minimal duration, here $m_e = 10$ ms, in segments shown by the bars across the curve representing $\log_{10} H_e$. Step 7: In each qualifying segment the maximum of $\underline{\mathbf{A}}^2(t)$ and its time of occurrence, t_{\max} , were calculated (triangles). The 1x64 feature vector used for classification of each AM pattern by the Hilbert method was given by the 64 values of peak power.

Step 4: The Hilbert transform was applied with a Hanning window to the EEG from every channel on each 6 s trial after spatial and temporal filtering to get the analytic amplitudes, $A_j(t)$, $j = 1, 64$. The square of the analytic amplitude was calculated at each digitizing step, t , on all channels, $j = 1, 64$. The mean square, $A_j^2(t)$, was calculated for the time series on each channel over the duration a moving window, w_e , that was centered at each digitizing step [see Table 1.1 in Freeman, 2004a for notation]. The 64 mean squared amplitudes formed a 64x1 feature vector, $\mathbf{A}^2(t)$, which specified the AM spatial pattern at that time, t , as a point in 64-space. The arithmetic mean of the 64 values, $\underline{\mathbf{A}}^2(t)$, expressed the normalized energy of the AM pattern (Fig. 1, B, lower trace).

Step 5: The frame given by each feature vector, $\mathbf{A}^2(t)$, was renormalized by dividing its 64 values by the mean, $\underline{\mathbf{A}}^2(t)$. The increment with each time step in renormalized spatial pattern was a scalar, $D_e(t)$, that was calculated by the Euclidean distance between successive pairs of points in 64-space at t and $t-1$. This parameter showed periods of large rates of change in spatial patterns

(Fig. 1, C) that bracketed periods of low rates of change indicating episodic pattern stability [Freeman, 2004a].

Step 6: The quantity termed ‘pragmatic information’ and denoted H_e was given by the ratio of the pattern intensity to the rate of pattern change estimated from the difference in normalized patterns [Freeman, 2004a]:

$$H_e = \underline{A}^2(t) / D_e(t). \quad (1)$$

High values of H_e (Fig. 1, D) reflected steps at which the rate of pattern change was low and the pattern intensity was high. Time series plots showed occasional high peaks having long duration that emerged from a highly irregular baseline. Displays of the time series (Fig. 1, D) and the distributions were facilitated by plotting the values of $\log_{10}H_e$ [Freeman, 2004a]. Peaks for H_e were located by setting a threshold value, t_e . A peak began when H_e rose above t_e and ended when it fell below t_e . Some minimal duration, m_e , was required to remove peaks that proved to be too brief to have informational value.

Step 7: The classification by nonlinear mapping was done using the feature vectors specified by the normalized patterns of analytic amplitudes squared, $\underline{A}^2(t)$, at the time points of maximal mean vector length, $\underline{A}^2(t)$.

Thus the parameters to be optimized were the temporal and spatial cut-off frequencies, the window, w_e , the threshold, t_e , and the minimal duration, m_e . Starting guesses were provided by preliminary analyses. Optimal values were found by constructing tuning curves (Fig. 2, A), in which a selected parameter was varied in small steps across an appropriate range, and the

number of correctly classified frames in the session was calculated at each parameter step in search of the maximum number. A single criterion was adopted by combining the three 64x1 feature vectors from the first 3 frames into a 192x1 vector that specified a single point in 192-space for each trial (Fig. 2, B). Any trial in which there were less than 3 frames in the control period or test period was omitted. If more than two trials were defective, that value of the parameter was disallowed. This method was also used to optimize spatial and temporal filters for each subject, as previously described in detail [Fig. 3 in Freeman, Burke and Holmes, 2003]. Each tuning curve was computer-intensive; a Macintosh G4 Powerbook required about 14 hours to complete the calculations for each session for one subject, so the method allowed variation of only one parameter in a run.

Preliminary assays on the present data showed that two pass bands were optimal, covering and extending beyond the beta range (8-40 Hz) and the gamma range (20-80 Hz). The window, w_e , was fixed at 64 ms for the gamma band and at 80 ms for the beta band, while the minimal duration, m_e , was fixed respectively at 20 ms for gamma and 30 ms for beta in all cases. Then the most critical parameter that required individuation, the threshold t_e , was evaluated for each case and pass band (Fig. 2, A). Given that value as an initial guess, the three screening parameters, window duration, w_e , minimal duration, m_e , and information threshold, t_e , were fine-tuned by constructing a 3x3x3 tensor with an optimized value at the center and 26 values $\pm 50\%$ of the center value and repeating the nonlinear mapping and classification procedures 27 times to employ all combinations, followed by selection of the triad with the highest number of correct classification for the 192x1 feature vector. This fine-tuning also required about 14-16 hours for each subject and trial set. The outcome was a set of EEG segments designated by start latency

and duration that were designated as frames in respect to the cinematographic hypothesis. After parameter optimization using the 192x1 feature vectors, the final step was to determine whether preprocessing the frames with Sammon's algorithm could help to reveal the high level of information in the 64x1 feature vectors by classifying the 3 frames on each trial with respect to the presence of a CS+ or CS- on randomly alternated trials.

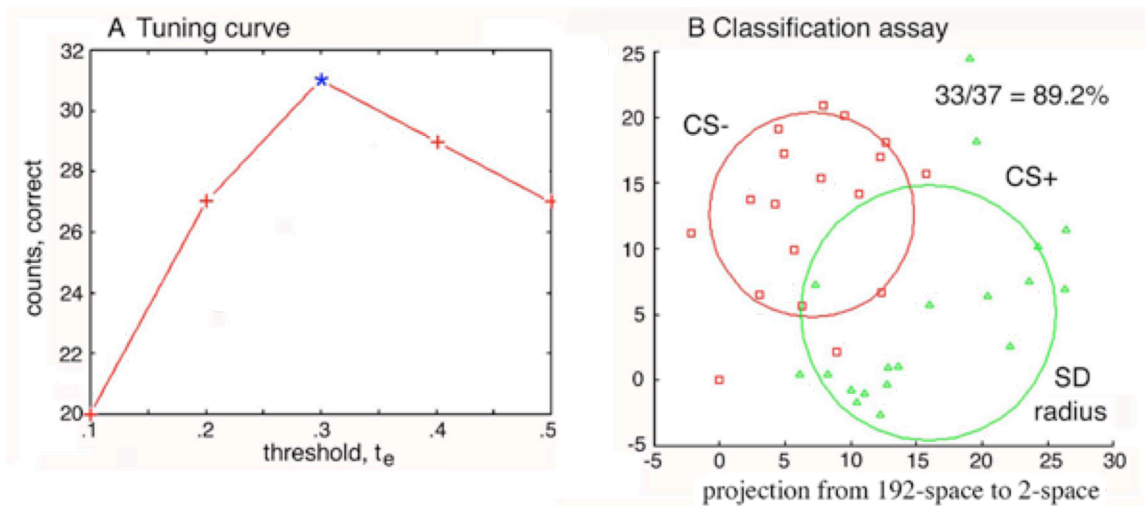


Fig. 2, A. The method for optimizing the threshold, t_e , is demonstrated.

B. The multidimensional scaling technique of nonlinear mapping [Sammon, 1969] projected clusters from 64-space into 2-space, optimizing their separation while preserving the relative distances between all of the data points. Two clusters were specified in this example: the 1x192 feature vector from the first three 1x64 feature vectors in the CS+ trials, and the 1x192 feature vector from the first three 1x64 feature vectors in the CS-. The circles representing the standard deviations (SD) of the clusters were calculated in the display plane.

2.3. Classification by Euclidean distance or by Sammon's nonlinear mapping

Classification in preceding studies was by the Euclidean distance method applied to rms amplitudes of fixed-length segments in a moving window time-locked across all trials, which required division of a session set into even and odd trials: a training set to calculate two centers of gravity and a test set to calculate the distance in n-space of each point to the two centers, then

repeating with reversal for cross-validation. Classification was judged to be correct when the distance of a frame on a CS+ trial was shorter to the CS+ center than to the CS- center, and so on. The binomial probability was used to compute the likelihood that the number of correct frames out of the total number of frames could have occurred by chance. This method was limited to two clusters and gave no visualization of the distributions of points.

The alternative method selected for preprocessing prior to classification was by nonlinear mapping [Sammon, 1969]. The mapping worked unsupervised to project the N points in L -space ($L = 192$ or 64) representing the whole set of N frames into a visualization plane for display, while preserving to a good approximation the distances between the points. An initial plane was defined by the two coordinate axes with largest variances of the data. The $N(N - 1)/2$ Euclidean distances were calculated between the points in L -space and between the points projected into the plane. An error function was defined by the normalized differences between the two sets of distances. The error was minimized by a steepest gradient descent procedure [equation (1) and Appendix 1 in Sammon, 1969].

After optimization the two sets of twenty 192×1 points representing frames were labeled by type of CS (+, -) and the six sets of twenty 64×1 points were labeled by CS type and sequential order (1, 2, 3). The center of gravity was calculated for each cluster (the centers of the two circles in Fig. 2, B). Classification of each point was by its Euclidean distance in the projection to the nearest center of gravity. The classification was correct when the type of the closest center in 2-space corresponded to the same type of frame. For a set of 20 trials of each type the results were expressed as % correct classification [Viana Di Prisco and Freeman, 1985; Barrie, Holcman and

Freeman, 1999]. An example of the output of Sammon's algorithm is shown in Fig. 2, B, where the circles indicate the SD of the radial coordinates within a cluster measured with respect to the center, and each point represents a 192x1 vector in 192-space for the itinerant trajectory formed by the first three post-stimulus frames in each trial (Fig. 3). Sammon's method gave flexibility in choosing the number of groups to be classified and the latencies and durations of temporal windows. However, it distorted the apparent Euclidean distances in deriving the clusters, so that comparison of centers from test and training subsets was unreliable. The level of significance for correct classification was evaluated by applying the same test to the 192x1 vector of the first three frames starting after 1.0 s in the pre-stimulus control period. Classification in the test period was considered to be significant if it exceeded the maximum of "correct" classification in the control period from all subjects and sessions as an estimate of $p < .01$. Both methods were applied to a representative session from every subject giving comparable levels of classification and significance, so only the results from Sammon's method are presented here.

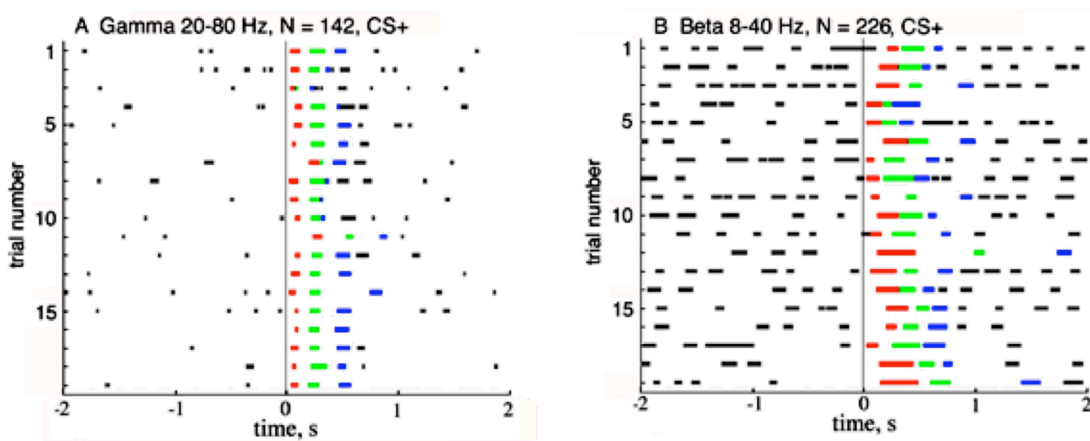


Fig. 3. The first 3 frames in a set of trials are labeled by color: first, red; second, green; third, cyan. The alignment of the segments in multiple columns just after CS onset at 3 s was most prominent in data from visual cortex with full-field flash but was not found in 1 of 3 somatic subjects nor in 2 of 4 auditory subjects with topographically delimited CS.

2.4. Estimation of duration and diameter of optimized frames

The durations of the 3 sequential frames were determined from the crossings of the trajectory, H_e over the threshold, t_e . An estimate of the diameters of these frames was obtained by fitting a cone to their analytic phase surfaces [Freeman, 2004b, Appendix 2, B]. The filtered EEG gave the real part of the time series on each channel; the Hilbert transform [Freeman, 2004a, Appendix 1, C] gave the imaginary part. The sum of squares of the real part and imaginary part at each point of maximal information, H_e , gave the 64×1 components of the feature vectors, $\mathbf{A}^2(t)$; the arctangent of the ratio of the imaginary part to the real part gave the analytic phase in radians at each of the 64 recording sites. The conic surface was fitted to the analytic phase; the slope of the cone gave the phase gradient in radians/mm. The reciprocal of the gradient gave the spatial wavelength in mm/cycle. Multiplying the wavelength by $\pi/4$ gave the diameter at half-power, which was adopted as a measure of the soft boundary condition for the interactive cortical domain that supported the spatially coherent carrier oscillation of the AM pattern in each frame.

3. Results

3.1. Classification with respect to CS+/- using the 192x1 feature vectors

Temporal pass bands of 20-80 Hz and 8-40 Hz with sets of optimized values for w_e and m_e were adopted for all trial sets (Table 1), and optimal values were found for t_c (Fig. 2, A). The two sets of correct classification values of CS+ vs. CS- for the 12 trial sets listed by cortex showed separation of 192x1 feature vectors for both pass bands in the three cortices, most strongly for visual cortex and least for auditory cortex. Minor adjustments in the parameters were made as noted in Table 1. Control segments were the first three frames in the pre-stimulus period starting 2 s before the CS onset. Statistical significance of the differences between control and test frames was evaluated by one-tailed t-test applied to the 12 group means.

Table 1. Correct classification of frames with optimized threshold

Cortex ms	Gamma 20-80 Hz, $w_e = 128$ ms, $m_e = 20$ ms					Beta 8-40 Hz, $w_e = 160$ ms, $m_e = 30$				
	t_e	#c/#tot	test	control	diff	t_e	#c/#tot	test	control	diff
Visual										
F152x10	0.3	33/37	89.2	56.8	32.4	2	31/37	83.8	59.5	24.3 [#]
F152x12	0.5	31/39	79.5	53.8	25.7	7	30/39	76.9	59.0	17.9
F9520x9	0.1	31/40	77.5	55.0	25.0 [^]	3	29/40	72.5	57.5	15.0
F9520x10	0.2	28/40	70.0	57.5	12.5 [”]	1	29/40	72.5	52.5	20.0
Avg	0.2		79.0	55.8	23.2	3		76.4	57.1	19.3
Somatic										
F528x2	1	26/40	65.0	50.0	15.0	2	27/40	67.5	65.0	2.5
L531x6	3	28/38	73.7	63.2	10.5	6	31/38	81.6	60.5	21.5
F220x4	4	30/40	75.0	45.0	30.0	14	29/40	72.5	62.5	10.0
F220x3	4	28/40	70.0	62.5	7.5	5	28/40	70.0	65.0	5.0
Avg	3		70.1	55.2	14.9	7		72.9	63.2	9.8
Auditory										
F553x3	0.1	24/40	60.0	57.5	2.5	3	31/40	77.5	67.5	10.0
F587x1	0.3	25/40	62.5	55.0	7.5 [^]	2	27/40	67.5	55.0	12.5
L530x2	1	28/40	70.0	70.0	0.0	5	30/40	75.0	60.0	15.0
L532x3	3	27/40	67.5	55.0	12.5	2	29/40	72.5	57.5	15.0
Avg	1		65.0	59.4	6.6	3		73.1	60.0	13.1
Average	1.5	28/39	71.7	56.8	14.9 [*]	4.3	29/39	74.2	60.1	14.1 ^{**}

[#] 8-32 Hz “ $m_e = 3$ [^]gap = 40 ms ^{*}p = 0.0002 ^{**}p = 0.000006

Table 1. Comparison of correct classification of control vs. test frames after optimizing temporal pass bands, values of threshold, t_e , window duration, w_e , and frame duration, m_e .

3.2 Classification of serial AM patterns with respect to CS+/-

The hypotheses were proposed on the basis of results from the Euclidean distance method [Barrie, Freeman and Lenhart, 1996] that three distinctive spatial AM patterns followed onset of

either the CS+ or CS-, and that on every trial each class of AM pattern would occur once and only once (Fig. 3). The hypotheses were tested by nonlinear mapping of the 6 groups corresponding to the first three 64x1 feature vectors appearing after each type of CS (Fig. 4, control A, test B). The same parameters were used as those listed in Table 1. The correct classification values of CS+ vs. CS- for each point with respect to the 6 centers of gravity were compared for the 3 test frames against the 3 control frames, from which differences were assessed as significant for the gamma range at $p < .05$ and for the beta range at $p < .01$ (Table 2, first column). The 12 trial sets showed significant classification of feature vectors only for the first frame in the gamma range and not for the second and third frames. In the beta range significant correct classification was found only in the third frame and not in the first two frames. Comparisons between successive frames revealed significant differences between the first, second and third frames for the CS- only for the gamma band, whereas the only successive difference for the beta band was that between the second and third frames for the CS+.

Table 2. Classification by frames, Mean \pm Standard Error of correct classification

A. Frames	6 centroids	CS-1 vs CS+1	CS-2 vs CS+2	CS-3 vs CS+3
Gamma				
Control	27.1 \pm 0.8	58.0 \pm 2.0	60.5 \pm 2.2	63.5 \pm 1.4
Test	30.2 \pm 1.7	68.2 \pm 3.2	60.6 \pm 2.3	57.0 \pm 2.2
Test-Control	3.1	10.1	0.1	-6.5
p	0.024	0.017	ns	ns
Beta				
Control	22.4 \pm 1.0	60.6 \pm 1.1	58.0 \pm 1.8	55.2 \pm 1.2
Test	27.1 \pm 0.8	58.0 \pm 2.0	60.9 \pm 1.7	65.2 \pm 55.2
Test-Control	4.7	-2.6	2.9	10.0
p	0.005	ns	ns	1.45E-05
B. Frames	CS-1 vs CS-2	CS-2 vs CS-3	CS+1 vs CS+2	CS+2 vs CS+3
Gamma				
Control	58.8 \pm 2.1	59.5 \pm 1.0	61.0 \pm 2.2	58.3 \pm 1.3
Test	65.7 \pm 2.4	69.1 \pm 3.2	60.1 \pm 2.2	56.6 \pm 1.8
Test-Control	6.9	9.6	-0.9	-1.7
p	0.024	0.009	ns	ns
Beta				
Control	56.4 \pm 1.4	57.8 \pm 2.3	59.2 \pm 1.4	58.8 \pm 1.4
Test	58.8 \pm 2/1	59.5 \pm 1.0	63.5 \pm 3.0	62.5 \pm 2.2
Test-Control	1.4	1.7	4.7	3.7
p	ns	ns	ns	0.048

N= 12, d.f. = 11 for one-tailed paired t-test

Table 2, A. Comparison of correct classification of CS+ vs. CS- for the first three frames in the gamma band (first rows) and the beta band (second rows).

B. Comparison of correct classification of sequential 2 pairs of frames for CS+ and for CS- in the gamma band (third rows) and the beta band (fourth rows).

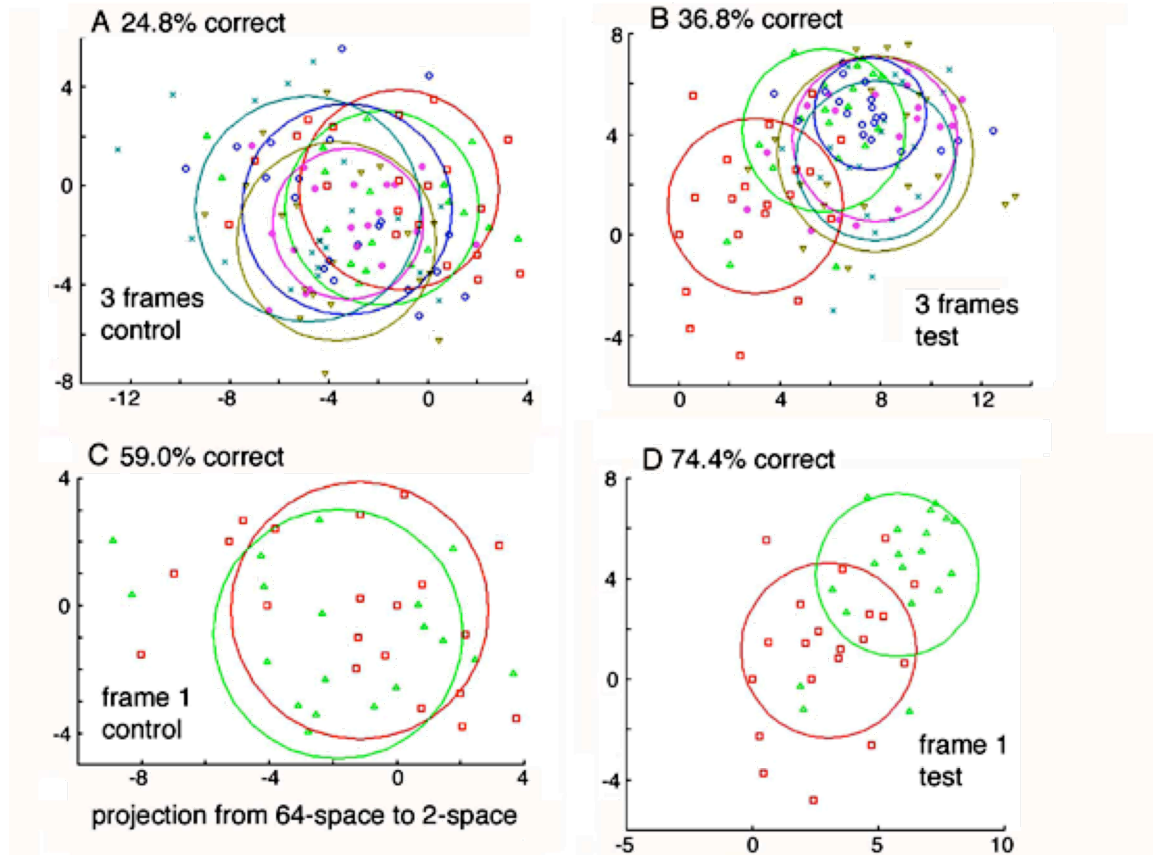


Fig. 4. **A.** Display of all groups, control. **B.** Display of all groups, test. **C.** First frame, control. **D.** First frame, test.

3.3. Measurement of the parameters of frames: control versus test

Start latencies ranged from 20-550 ms. The mean start latencies of the first control frames, 32-39 ms, averaged less than half the expected values, which were half the mean interval ranging from 156-214 ms. The mean start latencies of the first test frames, 65-66 ms, were consistent with the known mean start latencies of neocortical evoked potentials. The latencies of the second and third test frames exceeded those in the control frames in the gamma range but not in the beta range. The recurrence rates from the reciprocals of the mean intervals were in the higher half of the theta range for the gamma band and in the lower half for the beta band. There were no differences between CS+ and CS- frames, so the data were pooled for these statistics.

Durations ranged from 30-90 ms. Durations of the first test frames in both pass bands exceeded those of the first control frames. The durations of successive test frames in both pass bands decreased with increasing latency but not so of control frames (ANOVA $df = 2$, $F = 4.33$, $p = 0.014$). Diameters ranged from 10-36 mm, with frames in the beta range consistently exceeding those in the gamma range. There were no significant differences between successive frames or between CS+ and CS-. Peak power normalized with respect to the global mean of EEG from each trial set ranged from 0.07-0.60 SD. Normalized peak power in all test frames exceeded 2-fold that in all control frames in both pass bands. For test frames but not for control frames in the gamma range there was a decrease in peak power from the first to the second frame ($p < .05$); in the beta range for both CS- and CS+ a comparable decrease in peak power occurred from the second to the third frame ($p < 0.001$), bringing peak power to the control level. The data are summarized in graphic form in Fig. 5.

Table 3. Parameters of frames: mean \pm Standard Error (SE)

Pass band Frame	Gamma 20-80 Hz			Beta 8-40 Hz		
	first	second	third	first	second	third
Latency, ms						
Control	32 \pm 5	173 \pm 21	316 \pm 31	39 \pm 8.6	271 \pm 22	472 \pm 37
Test	66 \pm 16	239 \pm 31	406 \pm 35	65 \pm 8.8	268 \pm 19	490 \pm 47
Difference	34	65	92	26	-3	-18
p T > C	0.049	0.049	0.048	0.040	ns	ns
Duration, ms						
Control	42.1 \pm 2.8	38.6 \pm 3.3	39.5 \pm 2.9	71.8 \pm 5.2	65.8 \pm 4.2	67.8 \pm 3.1
Test	57.2 \pm 5.7	48.2 \pm 6.8	47.0 \pm 8.0	80.6 \pm 5.7	74.6 \pm 7.2	64.7 \pm 3.3
Difference	15.1	9.6	7.5	9.8	8.8	-3.1
p T > C	0.0002	0.024	ns	0.016	ns	ns
Diameter, mm						
Control	16.7 \pm 2.4	18.5 \pm 3.1	18.9 \pm 2.9	26.8 \pm 4.5	22.4 \pm 4.2	24.0 \pm 4.5
Test	18.3 \pm 3.0	16.8 \pm 3.0	18.6 \pm 3.5	21.6 \pm 4.1	25.9 \pm 5.5	25.3 \pm 4.7

Difference	1.6	-1.7	-.3	-5.2	3.5	1.3		
p T > C	ns	ns	ns	ns	ns	ns		
Peak power, A ² , normalized with respect to global SD x1000								
Control	88 ± 18	80 ± 17	83 ± 17	273 ± 32	256 ± 32	275 ± 41		
Test	173 ± 32	137 ± 37	143 ± 37	401 ± 46	417 ± 95	288 ± 47		
Difference	85	57	60	28	161	13		
p T > C	0.0001	0.043	0.032	0.004	0.012	ns		
Intervals, ms	141	143	142	(7.0 Hz)	232	201	216	(4.6 Hz)
	173	167	171	(5.8 Hz)	203	222	212	(4.7 Hz)
			156	(6.4 Hz)			214	(4.65 Hz)

Table 3. Pooled estimates are given of the latency, duration, diameter and peak power of the frames derived using the optimized values of the threshold, t_c , given in Table 1.

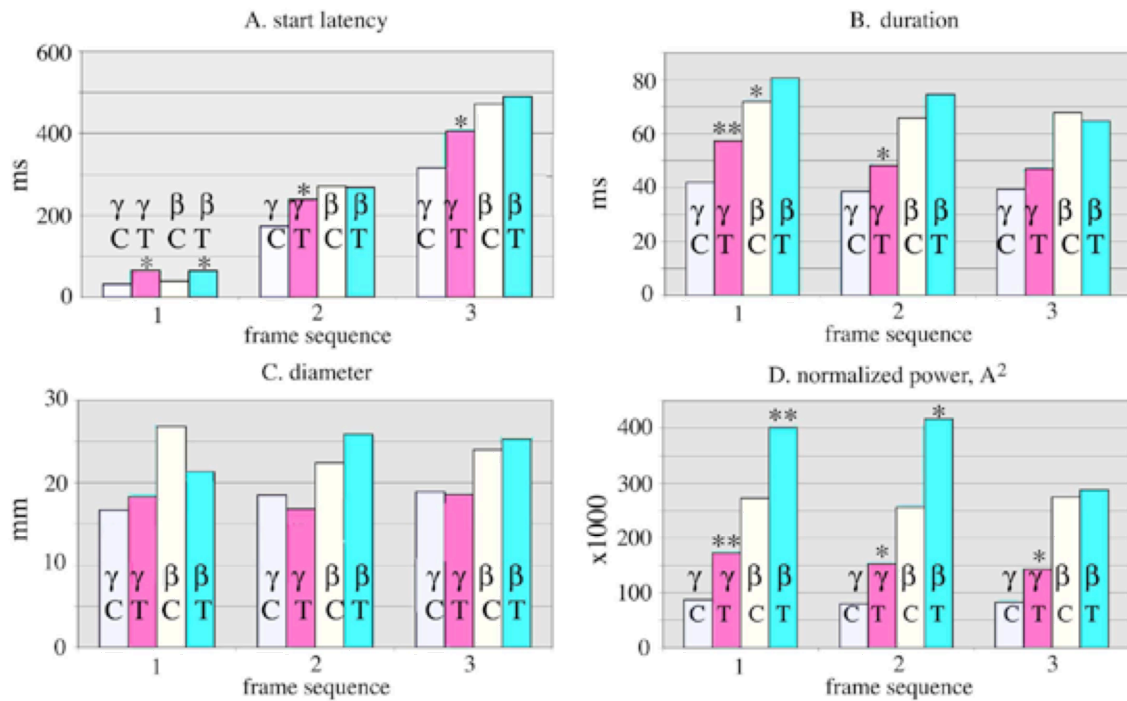


Fig. 5. The data in Table 3 are presented in graphic form.

A further test was conducted to determine whether the information in the data that served for classification was concentrated in any smaller number than the set of 64 channels. As in prior studies [Freeman and Baird, 1987; Barrie, Freeman and Lenhart, 1996; Freeman and Burke, 2003; Ohl, Deliano, Scheich and Freeman, 2003] the test was conducted by randomly deleting channels in varying numbers and repeating the classification test, while keeping an account of the contribution by each remaining channel. With one exception the results of prior studies were replicated in the present study; no channel was any more or less of value than any other, while the best classification rate was achieved by using all available channels. The exception was that in a study of the auditory cortex Ohl, Deliano, Scheich and Freeman [2003] found tonotopic specificity in the first classification peak.

4. Discussion

4.1 *The cinematographic hypothesis for study of AM patterns*

Sacks [2004] recently described reports by patients suffering migraines and Parkinson's disease of rare episodes in which their slowed perceptions broke into freeze-frames. From these descriptions and from his review of books on consciousness he concluded: "The *mechanism of our ordinary knowledge is of a cinematographical kind.*" His findings were preceded by half a century of researches that were triggered by the discovery of the alpha rhythm, which led several psychophysicologists [e.g., Walter, 1963] to propose that it manifested a scanning or gating mechanism by which visual awareness was parsed into frames. Explorations over the years have remained inconclusive.

Recent analyses of human scalp EEG using the Hilbert transform [Freeman, 2003; Freeman, Burke and Holmes, 2003] have provided electrophysiological evidence complementing previous analyses of animal data for repetitive phase transitions in neocortex at recurrence rates in the theta and alpha ranges. These phase transitions appear to segment the EEG into frames. If the cinematographic hypothesis is to be tested physiologically, some of the corollary questions should be: What are the properties of the frames? How many screens are there? How can the contents of frames be measured? What are the neural mechanisms by which frames are formed and by which their contents are transmitted and integrated?

The index for pragmatic information, H_e , appears well suited as a tool for locating frames in the EEG, because it selects segments in the filtered EEG that are characterized by intense multineuronal dendritic current that is likely to be accompanied by high density of neural firing. The segments defined by H_e also have high degrees of synchrony in beta or gamma oscillation; they cover spatial domains extending over several square cm; and they have stable spatial patterns of neural activity that persist for several tens of ms, typically 3-5 cycles of the peak carrier frequency [Freeman, 2004b]. By these criteria the H_e segments are likely to contain the organized neural activity that supports the stages of generalization, abstraction, and categorization in perception leading to recognition and recall. One form of requisite experimental proof is the demonstration of significant rates of correct classification of segments with respect to antecedent CS+/-, in order to infer that they are frames in the perceptual process invoked by conditioning. While the rates achieved in the present study are well above chance levels and indeed superior to prior results, they fall considerably short of the crispness that will be desired of a tool for analysis of the mechanisms of human perception. However, this first glimpse into the inner dynamics of perception at the level of the primary sensory cortices does offer some insights that may help substantially in devising further experimental exploration, as well as opening new avenues for theoretical explanation and modeling.

These new data support the concept that perception has two main stages: initial destabilization of a primary receiving area by sensory input that leads to formation of a local AM pattern ['wave packet', Freeman, 1975/2004, 2003c] having a carrier frequency in the gamma range; and subsequent emergence by self-organization of a global AM pattern having a carrier frequency in the beta range. The first stage of this sequence was most clearly seen here in the visual cortical data. The second, global stage has been documented by simultaneously recording in multiple sensory areas and the entorhinal cortex, showing that the first stage was not manifest in those

data, but that 2-4 peaks of multicortical AM pattern classification recurred later in the CS-CR interval [Freeman, Gaál and Jornten, 2003; Freeman and Burke, 2003]. The goodness of classification was reduced by removal of the data from each contributing brain area, which demonstrated that the spatial patterns were indeed multicortical. Measurement of the phase relations among the 5 areas showed that the global patterns formed by abrupt, transient increases in phase locking among the 5 areas [Freeman and Rogers, 2003].

The most notable deficiency of the present results was the poor level of classification in the auditory cortical data (Fig. 3). One explanation for the high failure rate for classification of early auditory AM patterns was the tonotopic restriction of the auditory CS to 500 and 5000 Hz tones, which stood in contrast to the full-field weak and stronger flashes in vision and the relatively broadly distributed air puffs to the face or back for somesthesia. The arrays were surgically placed over the sensory areas as described in the literature for the rabbit but without topographic testing with specific CS+/- prior to fixation [Barrie, Freeman and Lenhart, 1996]. The experiment was repeated in gerbils with meticulous location of an electrode array over the primary auditory area [Ohl, Scheich and Freeman, 2000], leading to clear identification of category learning [Ohl, Scheich and Freeman, 2001] that followed tonotopic spatial patterns.

Another limitation in the present study was the lack of a specific test for the extent to which the hypothesis held that one and only one frame of a given category occurred and could be detected on every trial. This aspect is still under investigation.

4.2. Interpretation of AM patterns in the perceptual process

A salient problem in perception is how to characterize the pre-stimulus background in two aspects. One aspect concerns the repeated state transitions that generate patterns of phase modulation in the form of cones. These phase cones are found by measuring spatial phase gradients [Freeman, 2004b] and are associated with recurrent AM patterns, and they have parameters of size and duration that conform to power law distributions. They appear to provide for the meta-stability of neocortex in a state of self-organized criticality [Freeman, 2004a]. Yet most of their AM patterns have as yet no detectable relation to specific stimuli or overt behaviors. The other aspect is the on-going life of each subject, in which it is to be presumed that, prior to the CS arrival, each primary sensory cortex contributes to brain states of awareness that might have little relevance to accessible parameters of behavioral observation and control except in terms of focused attention and expectancy. These on-going patterns of coordinated analytic phase differences (CAPD) are found by measuring the temporal phase gradients [Freeman, 2004a]. The independence of the spatial and temporal gradients (frequencies) has been well documented [Freeman, 2004b].

Expectancy might become apparent on comparing the AM pattern sequences following CS+ versus CS-. The present analysis contrasts the impact of an expected CS+ with that of a known CS-. Both induce early formation of an AM pattern that is focused in the pertinent primary sensory cortex and includes several or all its parts, with brief duration and a carrier frequency mainly in the low gamma range. Several hundred ms after the CS+ follows an AM pattern that is not well classified. A third AM pattern follows with definitely larger size, longer duration, and a carrier wave in the beta range. In contrast to the impact of the CS+, the first AM pattern after the CS- onset is followed by a second AM pattern still with a gamma carrier frequency and a pattern

that clearly differs from the first in texture but not in size or duration. This second AM pattern may be related to response suppression rather than selection in a go-no go paradigm. A third AM pattern with a beta carrier, long duration, and large diameter differs from that in CS+ trials in the late range but not from the second CS- AM pattern, perhaps again relating either to response suppression or to return to a prior state of expectancy.

4.3. Significance for human studies

The best and perhaps most compelling reason to develop these arcane techniques of background EEG pattern analysis is to provide a platform on which to base comparable analyses of human scalp EEG, in order to take advantage of the cognitive and phenomenological skills of normal healthy subjects and their verbal descriptions of mental states. The question arises, whether the textures of Gestalt-related AM patterns might be detected from scalp recordings. Animal studies with simultaneous EEG recording from multiple cortices suggest a positive answer, from the intermittent high rates of classification that have been found in multicortical AM patterns formed by EEGs from five mini-arrays fixed on the visual, auditory, somatic, entorhinal cortices and the olfactory bulb [Freeman, Gaál and Jornten, 2003; Freeman and Burke, 2003]. Distances of one to four cm separated these arrays.

Estimates of the distances across which coherent states of beta and gamma activity form in human scalp EEG [Freeman, Holmes and Burke, 2003] show that multicortical AM patterns may be large enough to provide surface areas suitable for EEG pattern analysis from high-density scalp arrays. Repeated studies have shown that the classificatory information is distributed in the spatial frequency domain [Freeman and Baird, 1987; Ohl, Deliano, Scheich and Freeman, 2003; Freeman and Burke, 2003], so that the locations of electrodes in arrays need not be specified precisely, only that they not be moved during the course of a perceptual study. The minimum number of channels is about 16 [Barrie, Lenhart and Freeman, 1996; Ohl, Scheich and Freeman, 2001] though more is better. The best location on which to place a high-density array is the left or right calvarium with reference to the vertex in order to minimize interference from EMG [Freeman, Holmes, Burke and Vanhatalo, 2003]. In the absence of access to restricted topographic areas of primary sensory cortex the more useful CS may be broad and 'natural', as distinct from those with the narrow boundaries of spatial and spectral location that are needed for sensory analysis. Suggested tasks would require multisensory discrimination with formation of pairs of chaotic itinerant trajectories through brain state space [Tsuda, 2001], each with 2 or more stable brain states along the way.

References

- Atmanspacher H, Scheingraber H. Pragmatic information and dynamical instabilities in a multimode continuous-wave dye laser. *Can. J. Phys.* 1990, 68: 728-737.
- Barrie JM, Freeman WJ, Lenhart M. Modulation by discriminative training of spatial patterns of gamma EEG amplitude and phase in neocortex of rabbits. *J. Neurophysiol.* 1996, 76: 520-539.
- Barrie JM, Holcman D, Freeman WJ. Statistical evaluation of clusters derived by nonlinear mapping of EEG spatial patterns. *J Neurosci Meth* 1999, 90: 87-95.
- Engel AK, Fries P, Singer W. Dynamic predictions: oscillations and synchrony in top-down processing. *Nature Neurosci. Rev.* 2001, 2: 704-716.
- Freeman WJ. *Mass Action in the Nervous System*. Academic Press, New York, 1975. Reprinted 2004: <http://sulcus.berkeley.edu/MANSWWW/MANSWWW.html>
- Freeman WJ. *Neurodynamic. An Exploration of Mesoscopic Brain Dynamics*. Springer, London, 2000.
- Freeman WJ. A neurobiological theory of meaning in perception. Part 1. Information and meaning in nonconvergent and nonlocal brain dynamics. *Int. J. Bifurc. Chaos* 2003a, 13: 2493-2511.
- Freeman WJ. A neurobiological theory of meaning in perception. Part 2. Spatial patterns of phase in gamma EEG from primary sensory cortices reveal the properties of mesoscopic wave packets. *Int. J. Bifurc. Chaos* 2003b, 13: 2513-2535.
- Freeman WJ. The wave packet: An action potential for the 21st century. *J. Integrative Neurosci.* 2003d, 2: 3-30.
- Freeman WJ. Origin, structure and role of background EEG activity. Part 1. Analytic amplitude. *Clin. Neurophysiol.* 2004a, 115: 2077-2088.
- Freeman WJ. Origin, structure and role of background EEG activity. Part 2. Analytic phase. *Clin. Neurophysiol.* 2004b, 115: 2089-2107.
- Freeman WJ, Baird B. Relation of olfactory EEG to behavior: Spatial analysis: *Behav. Neurosci.* 1987, 101: 393-408.
- Freeman WJ, Barrie JM. Analysis of spatial patterns of phase in neocortical gamma EEGs in rabbit. *J. Neurophysiol.* 2000, 84: 1266-1278.
- Freeman WJ, Burke BC. A neurobiological theory of meaning in perception. Part 4. Multicortical patterns of amplitude modulation in gamma EEG. *Int. J. Bifurc. Chaos* 2003, 13: 2857-2866.
- Freeman WJ, Burke BC, Holmes MD. Aperiodic phase re-setting in scalp EEG of beta-gamma oscillations by state transitions at alpha-theta rates. *Hum. Brain Mapp.* 2003, 19: 248-272.
- Freeman WJ, Burke BC, Holmes MD, Vanhatalo S. Spatial spectra of scalp EEG and EMG from awake humans. *Clin. Neurophysiol.* 2003, 16: 1055-1060.
- Freeman WJ, Gaál G, Jornten, R. A neurobiological theory of meaning in perception. Part 3. Multiple cortical areas synchronize without loss of local autonomy. *Int. J. Bifurc. Chaos* 2003, 13: 2845-2856.
- Freeman WJ, Grajski KA. Relation of olfactory EEG to behavior: Factor analysis. *Behav. Neurosci.* 1987, 101: 766-777.
- Freeman WJ, Rogers LJ. Fine temporal resolution of analytic phase reveals episodic synchronization by state transitions in gamma EEGs. *J. Neurophysiol.* 2002, 87: 937-945.

- Freeman WJ, Rogers L.J. A neurobiological theory of meaning in perception. Part 5. Multicortical patterns of phase modulation in gamma EEG. *Int. J. Bifurc. Chaos* 2003, 13: 2867-2887.
- Freeman WJ, Rogers LJ, Holmes MD, Silbergeld DL. Spatial spectral analysis of human electrocorticograms including the alpha and gamma bands. *J. Neurosci. Meth.* 2000, 95: 111-121.
- Grajski KA, Freeman WJ. Spatial EEG correlates of nonassociative and associative olfactory learning in rabbits. *Behav Neurosci* 1989, 103: 790-804.
- König A. Interactive visualization and analysis of hierarchical neural projections for data mining. *IEEE Trans. Neural Networks TNN* 2000, 11: 615 - 624.
- Kozma R, Freeman WJ. Chaotic resonance: Methods and applications for robust classification of noisy and variable patterns. *International Journal of Bifurcation and Chaos* 2001, 10: 2307-2322.
- Ohl FW, Scheich H, Freeman WJ. Topographic analysis of epidural pure-tone-evoked potentials in gerbil auditory cortex. *J. Neurophysiol.* 2000, 83: 3123-3132.
- Ohl FW, Scheich H, Freeman WJ. Change in pattern of ongoing cortical activity with auditory category learning. *Nature* 2001, 412: 733-736.
- Ohl, FW, Deliano M, Scheich H, Freeman WJ. Early and late patterns of stimulus-related activity in auditory cortex of trained animals. *Biol. Cybern.* 2003, 88: 374-379.
- Sacks O. In the river of consciousness. *New York Review* 2004, 51: Number 1, January 15.
- Sammon JW. A nonlinear mapping for data structure analysis. *IEEE Trans. Comput.* 1969, C-18: 401-409.
- Singer W, Gray CM. Visual feature integration and the temporal correlation hypothesis. *Ann. Rev. Neurosci.* 1995, 18: 555-586.
- Tallon-Baudry C, Bertrand O, Delpuech C, Pernier J. Stimulus-specificity of phase-locked and non phase-locked 40-Hz visual responses in human. *J. Neurosci.* 1996, 16: 4240-4249.
- Tsuda I. Toward an interpretation of dynamics neural activity in terms of chaotic dynamical systems. *Behav. Brain Sci.* 2001, 24: 793-847.
- Viana Di Prisco, Freeman WJ. Odor-related bulbar EEG spatial pattern analysis during appetitive conditioning in rabbits. *Behav Neurosci* 1985, 99: 964-978.
- Walter WG. *The Living Brain*. New York: Norton, 1963.